DOI: 10.1534/genetics.109.105254

Systems-Level Engineering of Nonfermentative Metabolism in Yeast

Caleb J. Kennedy,[1] Patrick M. Boyle,[1] Zeev Waks and Pamela A. Silver[2]

Department of Systems Biology, Harvard Medical School, Boston, Massachusetts 02115

Manuscript received May 20, 2009
Accepted for publication June 19, 2009

ABSTRACT

We designed and experimentally validated an *in silico* gene deletion strategy for engineering endogenous one-carbon (C1) metabolism in yeast. We used constraint-based metabolic modeling and computer-aided gene knockout simulations to identify five genes (*ALT2*, *FDH1*, *FDH2*, *FUM1*, and *ZWF1*), which, when deleted in combination, predicted formic acid secretion in *Saccharomyces cerevisiae* under aerobic growth conditions. Once constructed, the quintuple mutant strain showed the predicted increase in formic acid secretion relative to a formate dehydrogenase mutant (*fdh1 fdh2*), while formic acid secretion in wild-type yeast was undetectable. Gene expression and physiological data generated *post hoc* identified a retrograde response to mitochondrial deficiency, which was confirmed by showing Rtg1-dependent NADH accumulation in the engineered yeast strain. Formal pathway analysis combined with gene expression data suggested specific modes of regulation that govern C1 metabolic flux in yeast. Specifically, we identified coordinated transcriptional regulation of C1 pathway enzymes and a positive flux control coefficient for the branch point enzyme 3-phosphoglycerate dehydrogenase (PGDH). Together, these results demonstrate that constraint-based models can identify seemingly unrelated mutations, which interact at a systems level across subcellular compartments to modulate flux through nonfermentative metabolic pathways.

FORMIC acid is an important intracellular metabolite that has been adapted for specific functions in different organisms. It is produced and secreted in small amounts as a fermentation by-product by bacteria in the family Enterobacteriaceae (Leonhartsberger *et al.* 2002) and in large quantities as an irritant and pheromone by ants (Hefetz and Blum 1978). Formic acid is used commercially as a preservative in animal feed and has a potential use as a precursor to hydrogen, since it is one of only a few biological molecules with sufficient reducing potential (Milliken and May 2007). The main pathway for biohydrogen production during mixed acid fermentation in *Escherichia coli* proceeds through a formic acid intermediate: a product of the reaction catalyzed by pyruvate formate lyase (PFL) (EC 2.3.1.54) (Birkmann *et al.* 1987).

As yeast (and other eukaryotes) lack a PFL homolog, their primary source of formic acid is through tetrahydrofolate (THF)-mediated one-carbon (C1) reactions present in the mitochondria (McNeil *et al.* 1996). In mammalian cells C1 metabolism is responsible for up to 90% of single carbon units required for nucleotide biosynthesis (Fu *et al.* 2001). The first reaction in this pathway is catalyzed by the branch point enzyme 3-phosphoglycerate dehydrogenase (PGDH) (EC 1.1.1.95) encoded by the yeast isozymes *SER3* and *SER33*. The NAD-dependent oxidation reaction catalyzed by PGDH is nonfermentative: oxygen, rather than organic substrate, acts as the final electron acceptor to maintain redox homeostasis under conditions where high levels of serine and formic acid are synthesized from the glycolytic intermediate 3-phosphoglycerate (3PG) (Peters-Wendisch *et al.* 2005).

Constraint-based (stoichiometric) models are capable of describing systems-level properties of metabolic networks without requiring specific information about molecular mechanism or reaction-specific kinetics. As many of these parameters are often unknown, constraint-based methods have advantages over their kinetic counterparts as practical tools for developing systems-level metabolic engineering strategies. These models rely on well-annotated genomic sequences to define sets of metabolites and the stoichiometric matrix of known biochemical reactions. Once these are defined, feasible assumptions about quasi-steady-state optimality are all that is necessary to predict reaction rates for the entire system. Combinatorial enzyme deletion phenotypes can be explored systematically by constraining specific enzyme-reaction fluxes to zero (for example, Edwards and Palsson 2000; Forster *et al.* 2003). This approach provides reasonable approximations of genomewide biochemical processes in several model organisms (Edwards and Palsson 2000; Duarte *et al.* 2004; Bro

Supporting information is available online at http://www.genetics.org/cgi/content/full/genetics.109.105254/DC1.

[1]These authors contributed equally to this work.

[2]*Corresponding author:* Department of Systems Biology, Harvard Medical School, 200 Longwood Ave., WAB 536, Boston, MA 02115.
E-mail: pamela_silver@hms.harvard.edu

et al. 2006; Hjersted *et al.* 2007; Oh *et al.* 2007; Resendis-Antonio *et al.* 2007; Becker and Palsson 2008; Motter *et al.* 2008).

Constraint-based methods provide a solid mathematical foundation for identifying important properties of biochemical pathways. Under a certain set of stoichiometric constraints, metabolic networks can be decomposed into a finite number of elementary flux modes (EFMs) or extreme pathways (Papin *et al.* 2002). The properties of EFMs have important biological implications. EFMs are the unique set of nondecomposable pathway flows for a given biochemical network (Schuster *et al.* 2000). In biological terms, EFMs are modular units of pathway function—minimal sets of enzymes required to catalyze whole metabolic reactions. Because metabolic pathways are highly integrated, the number of possible pathways connecting reactants and products grows exponentially. Thus EFM analysis is computationally tractable only for individual pathways or small metabolic subnetworks (Klamt and Stelling 2002).

Past metabolic engineering efforts in eukaryotic microbes have sought to control flux through anaerobic pathways for increased production of metabolites produced by fermentation. These include lactate (van Maris *et al.* 2004; Ishida *et al.* 2006), malate (Zelle *et al.* 2008), isoprenoids (Shiba *et al.* 2007; Herrero *et al.* 2008; Kizer *et al.* 2008), glycerol (Geertman *et al.* 2006; Cordier *et al.* 2007), and ethanol (Alper *et al.* 2006; Bro *et al.* 2006), among others. Although nonfermentative by-products represent a class of biologically interesting and commercially attractive small molecules, efforts aimed at engineering microbes for increased production of these metabolites are comparatively infrequent.

Reactions that produce the major one-carbon donors serine, glycine, and formic acid are often duplicated in the cytoplasm and mitochondrion (Christensen and Mackenzie 2006). Flux through these reactions is generally oxidative in the mitochondria and reductive in the cytoplasm; however, C1 metabolic pathways are under considerable regulatory control and can be adapted to specific genetic backgrounds and growth conditions (Kastanos *et al.* 1997; Piper *et al.* 2000). Two groups have independently shown that C1 enzymes are controlled dynamically by glycine at the transcriptional level. Upon glycine withdrawal many enzymes involved in C1 metabolism are strongly repressed, a regulatory event that requires the transcription factor Bas1 (Subramanian *et al.* 2005). Under conditions of glycine induction Gelling *et al.* (2004) noticed a similar pattern of C1 enzyme differential expression; however, Bas1 was not required for the observed effect in this case. In both of these studies the intact cytosolic serine hydroxymethyltransferase Shm2 (EC 2.1.2.1) was necessary for glycine-dependent changes in C1 enzyme expression (Gelling *et al.* 2004; Subramanian *et al.* 2005). Although contradicting evidence exists, results reported thus far demonstrate the dynamic control of C1 metabolism in eukaryotes.

To investigate metabolic engineering strategies for controlling biosynthetic flux through a nonfermentative pathway, we chose to construct strains of *Saccharomyces cerevisiae* that increase flux through C1 metabolism. We chose a constraint-based modeling approach to develop genetic engineering strategies leading to increased production of formic acid. We experimentally validated our modeling strategy and identified specific transcriptional control mechanisms that govern C1 metabolism in the engineered strain.

MATERIALS AND METHODS

Constraint-based modeling and *in silico* gene deletion: The validated, genome-scale metabolic model *S. cerevisiae* *i*ND750 previously described by Duarte *et al.* (2004) was used to model the fully compartmentalized yeast metabolic network. The flux balance analysis (FBA) optimization problem was formulated as described previously (Varma and Palsson 1994) in the GNU MathProg language and solved with custom-generated C code (available upon request), implementing the GNU linear programming (LP) kit (GLPK) available at ftp://aeneas.mit.edu/pub/gnu/glpk.

Specifically, we defined quasi-steady-state conditions using the yeast stoichiometric matrix S and unknown flux vector v,

$$S \cdot v = 0,$$

with maximization of growth rate (μ) as the objective function for FBA:

$$\max \mu$$
$$s.t.\ v_{\min,i} \leq v_i \leq v_{\max,i}.$$

Thermodynamic constraints in *i*ND750 are derived from the KEGG database (http://www.genome.jp/kegg/) and associated with individual reactions to define v_i^{ub} and v_i^{lb}, which are the upper and lower bounds of each reaction i. We modeled 20 mmol gDW^{-1} hr^{-1} constant glucose uptake, nutrient uptake fluxes appropriately constrained to simulate synthetic complete media including the addition of serine (Figure 1A; supporting information, Table S1), oxygen uptake flux that was either fixed to 0 mmol gDW^{-1} hr^{-1} or left unconstrained to simulate anaerobic or aerobic growth conditions, respectively, and internal fluxes constrained to $\{0, \infty\}$ or left unconstrained to simulate irreversible or reversible reactions, respectively. It is important to note that multiple optimal solutions are possible in which the objective function constraint is satisfied (Lee *et al.* 2000; Phalakornkule *et al.* 2001). We sampled alternative optimal solutions for the mutant strains predicted to increase flux to formic acid by relaxing the directionality constraint of individual reactions (Lee *et al.* 1997). Results from this analysis indicated some flexibility in the formic acid biosynthetic pathway; however, the three mutations *alt2*, *fum1*, and *zwf1* were consistently associated with significant increases in formic acid secretion, with a minimum secretion rate of 53.65 mmol gDW^{-1} hr^{-1} (other data not shown).

To identify the maximum theoretical yield for formic acid production we substituted formic acid secretion for biomass in the objective function. All the other constraints were appropriate for external exchange and aerobic growth. Maximizing this objective resulted in Equation 1, which can be considered

the "type I" through pathway for formic acid biosynthesis (Schilling *et al.* 2000).

Several efficient algorithms have been developed for identifying a single solution of optimal gene knockouts (for example, Burgard *et al.* 2003). We chose an iterative simulation strategy as we were interested in all combinations of gene knockouts predicted to affect C1 metabolism and formic acid production, including solutions that might be considered suboptimal under formal definitions. By constraining the fluxes of individual sets of ≤3 nonessential genes to zero and reevaluating the system using LP we simulated metabolic phenotypes for >4 million gene combinations in reasonable time frames (<4 hr on an x86-64 processor running Linux version 2.6.15-51). Our knockout simulation protocol is summarized with the following pseudocode:

$$
\begin{aligned}
p &\leftarrow \text{powerset}(\{\text{nonessential genes}\})\\
\text{for each combo} &\in p\text{: } |p| \le 3\\
\text{for each } c &\in \text{combo}\\
v_c^{\text{ub}} &= 0.0\\
v_c^{\text{lb}} &= 0.0.
\end{aligned}
$$

Yeast strains and plasmids: PSY3642 was derived from the *fdh1 fdh2* parental strain PSY3639 (Overkamp *et al.* 2002) by iterative gene replacement (Guldener *et al.* 1996). Briefly, LoxP-KanMX gene deletion cassettes for *ALT2*, *FUM1*, and *ZWF1* were generated by PCR, using primers with 45 bp of flanking homology and pUG6 as template (Guldener *et al.* 1996). KanMX$^+$ transformants were selected on YPD plates containing 200 mg/liter G418 (geneticin). After confirming integration by single-colony PCR, G418 sensitivity was reestablished for subsequent gene replacement by expressing Gal4-Cre from pSH65 (Guldener *et al.* 1996) and selecting transformants on YPD plates containing 50 mg/liter phleomycin. Correct excision of LoxP-KanMX was confirmed by single-colony PCR.

The biobrick assembly method (Knight 2003; Phillips and Silver 2006) was used to generate the expression plasmid pRS410a consisting of (ordered 5′–3′) the yeast *CUP1* promoter, the yeast Kozak sequence, the catalytic domain of SerA (cloned by PCR from *E. coli* genomic DNA), in-frame fusion of the V5 epitope, the stop codon, and the yeast *ADH1* terminator. The flanking biobrick restriction sites *Xba*I and *Spe*I were used to subclone the expression fragment into pRS410 (Addgene). Yeast transformants were selected on YPD plates containing 200 mg/liter G418 and cultured with the same concentration of drug in synthetic complete media containing 2% glucose and 0.3 mm $CuSO_4$. Primer sequences used in this study are shown in Table S3.

Metabolite determination: Extracellular formic acid and ethanol measurements were made using spectrometric enzymatic assays at 340 nm according to the manufacturer's specifications (R-Biopharm). Yeast cultures were grown in synthetic complete media with 2% glucose under batch conditions in baffled (aerobic) or round bottom (anaerobic) Erlenmeyer shaker flasks. Anaerobic cultures were grown in sparged media under nitrogen gas.

Samples for intracellular metabolite measurements were prepared, using several methods as conceptual frameworks (Lange *et al.* 2001; Visser *et al.* 2004; Canelas *et al.* 2008; Sporty *et al.* 2008). Briefly, 20-ml samples were quickly drawn at a log phase (cell density of 0.4–0.6 OD_{600}) and immediately quenched in 32 ml cold 60% (v/v) methanol. A frozen binary solution of 60% (v/v) ethanol was used to maintain the yeast samples and quenching solution at −40°. Two subsequent washes were performed using the cold quenching solution, followed by cell lysis at 4° using a glass bead beater in the presence of 75% (v/v) ethanol to precipitate proteins. Samples were lyophilized overnight, resuspended in 100 μl anaerobic water, and centrifuged twice before use. The supernatant was stored at −80° until processing via HPLC.

HPLC measurements were performed using a Waters 2695 HPLC separation module fitted with a Luna C18 5-μm column, 250 × 4.5 mm (Phenomenex). Samples of 75–85 μl were injected and eluted at a flow rate of 1 ml/min, starting with 100% mobile phase buffer A and gradually increasing to 100% mobile phase buffer B (Di Pierro *et al.* 1995). Specifically, the relative fraction of buffer B in the mobile phase was increased at a rate of 15%/min until 60%, at 0.6%/min until 80%, during which the majority of separation occurred, and at 20%/min until 100% was reached. Buffer A contained 10 mm tetrabutylammonium hydroxide, 10 mm KH_2PO_4, and 0.25% methanol at pH 7.0 (Di Pierro *et al.* 1995). Buffer B contained 2.8 mm tetrabutylammonium hydroxide, 100 mm KH_2PO_4, and 30% methanol at pH 5.5 (Di Pierro *et al.* 1995). NAD was analyzed at 260 nm, and NADH was analyzed at 340 nm using a photodiode array detector (Waters 996) (Di Pierro *et al.* 1995; Sporty *et al.* 2008). Standard curves of specific metabolites were performed to enable quantification.

Gene expression profiling and analysis: Poly(A) mRNA was obtained in biological triplicate by trizol extraction (Invitrogen, Carlsbad, CA) from early log-phase ($OD_{600} = 0.4$) yeast grown aerobically. cDNA was generated from PSY3642 and PSY3639 by reverse transcription, differentially labeled with Cy3 or Cy5, respectively (one sample was processed with the labeling reversed to minimize artifacts introduced by incorporation bias), and hybridized to whole-genome cDNA microarrays (http://www.microarray.ca/). Array scans were analyzed with GenPix software and Rosetta Resolver (complete data are available in Table S4).

Gene ontology enrichment was obtained using GoStat (http://gostat.wehi.edu.au/) with Benjamini false discovery to correct for multiple hypothesis testing. The query set for enzyme annotation analysis was limited to those gene identities with represented reactions in *i*ND750 for which flux values were calculated.

Hierarchical clustering was applied to genomewide expression profiles of PSY3642 (compared to PSY3639) and other genetic knockout strains (excluding overexpression and drug treatment conditions) in the compendium described by Hughes *et al.* (2006). Routines were implemented in R (http://www.r-project.org/) with a Euclidean distance metric and Ward's minimum variance clustering algorithm (Murtagh 1985).

We used YEASTRACT-DISCOVERER (http://www.yeastract.com/) to find transcription factor binding motif enrichments in the promoter regions of genes with significant activation ($P < 0.01$) greater than twofold (Teixeira *et al.* 2006; Monteiro *et al.* 2008).

Phenotypic analysis: Mitotracker Red CMXRos and Mitotracker CM-H_2XRos (Invitrogen) were used to stain mitochondria. CMXRos selectively stains mitochondria and fluoresces in the red portion of the spectrum. CM-H_2XRos is a reduced version of CMXRos and fluoresces only when oxidized in respiring mitochondria (Ludovico *et al.* 2002). Overnight yeast cultures were resuspended in YEPD media containing either 1 μm of CMXRos or 3 μm CM-H_2XRos and incubated at 30° for 30 min prior to imaging.

Antibodies and Western blotting: PVDF membranes were blocked with phosphate-buffered saline containing 0.25% Tween-20 (PBST) and 5% nonfat dry milk, probed with mouse monoclonal primary antibodies against actin (Chemicon) or V5 (Sigma, St. Louis) and appropriate HRP-conjugated

TABLE 1

Gene combinations affecting C1 metabolic flux and formic acid secretion identified through *in silico* knockout simulation

Rank	Genotype	Efficiency (%)[a]
1	*fdh1 fdh2 alt2 fum1 zwf1*	72.3
2	*fdh1 fdh2 aat2 fum1 zwf1*	72.2
3	*fdh1 fdh2 cat2 fum1 zwf1*	72.0
4	*fdh1 fdh2 cat2 fum1 rpe1*	71.7
5	*fdh1 fdh2 cat2 fbp1 fum1*	30.5
6	*fdh1 fdh2 cat2 yat2 slc1*	2.4
7	*fdh1 fdh2 cat2 yat2 cho1*	2.3
8	*fdh1 fdh2 cat2 yat2 alt2*	1.2

[a] One hundred percent efficiency is defined as four formic acid molecules per glucose.

secondary antibody (Jackson), washed with PBST, and developed with enhanced chemiluminescence substrate (Amersham, Piscataway, NJ).

RESULTS

Pathway analysis of C1 metabolism in yeast: We performed limited pathway analysis of the yeast metabolic network to identify Equation 1, which represents the complete oxidation of glucose into formic acid (see MATERIALS AND METHODS):

$$C_6H_{12}O_6 + 4O_2 \rightarrow 4HCOOH + 2CO_2 + 2H_2O + \text{energy}. \quad (1)$$

Due to the quasi-steady-state assumption, individual reaction rates in Equation 1 are likely to be correlated during C1-mediated formic acid secretion, a condition that strongly suggests coordinated regulation of enzymes in this pathway (SCHUSTER *et al.* 2002). Coregulation of enzymes involved in glycolysis is well characterized; however, it is not fully understood if and how endogenous transcriptional programs coordinate C1 metabolism to affect formic acid biosynthesis.

Theoretically, maximum flux through Equation 1 would result in four formic acid molecules per glucose, a twofold yield increase compared to PFL-catalyzed reactions associated with mixed acid fermentation in *E. coli* (BIRKMANN *et al.* 1987). This may have important biotechnological applications for biofuel production. Assuming 100% conversion of exogenous formic acid into hydrogen, a two-step conversion process using endogenous hydrogenases in *E. coli* could result in 4 H_2 per glucose (YOSHIDA *et al.* 2005; WAKS and SILVER 2009). Formic acid production in yeast is relatively low and secretion is essentially nonexistent (BLANK *et al.* 2005); however, there is reason to believe that engineering C1 metabolism to produce high levels of formic acid is achievable. Various insect species regulate homologous pathways to produce large quantities of formic acid for the purposes of defense and communication (HEFETZ and BLUM 1978).

TABLE 2

Yeast strains

Strain	Genotype[a]	Reference
PSY3639	*fdh1(41, 1091)::loxP fdh2(41, 1091)::loxP*	OVERKAMP *et al.* (2002)
PSY3640	*zwf1::loxP*	This study
PSY3641	*zwf1::loxP fum1::loxP*	This study
PSY3642	*zwf1::loxP fum1::loxP alt2::loxP*	This study
PSY3650	*zwf1::loxP fum1::loxP alt2::loxP rtg1::KanMX*	This study
PSY3653	*fum1::KanMX*	This study

[a] All mutations are present in the CEN.PK113-7D *MAT***a** URA3 HIS3 LEU2 TRP1 MAL2 SUC2 genetic background. PSY3640–PSY3642, PSY3650, and PSY3653 are derived from PSY3639.

A model-driven metabolic engineering strategy to increase endogenous formic acid secretion: To formulate genetic engineering strategies leading to increased production of formic acid in yeast, we used the compartmentalized metabolic model *i*ND750 (DUARTE *et al.* 2004) and an iterative gene knockout simulation strategy to identify combinatorial enzyme deletions predicted to significantly increase formic acid secretion (see MATERIALS AND METHODS for details). As an exhaustive screen through all triple-knockout combinations would have been experimentally infeasible, we used FBA to screen combinatorial knockouts *in silico*. We identified several gene knockout combinations, which predicted nonzero secretion rates of formic acid (Table 1). In all cases eliminating the NAD-dependent formate dehydrogenase (FDH) reaction (EC 1.2.1.2) was required for secretion of formic acid. This is not surprising as FDH is thought to protect yeast from formic acid toxicity by catalyzing its irreversible oxidation to CO_2 (OVERKAMP *et al.* 2002).

We chose to proceed by constructing the mutant strain predicted to have the highest formic acid production efficiency (Table 1). In addition to *FDH1* and *FDH2*, three other genes were targeted for mutation by serial gene replacement (Table 2): *ALT2*, a putative cytoplasmic alanine transaminase (EC 2.6.1.2); *FUM1*, fumarase (EC 4.2.1.2); and *ZWF1*, glucose-6-phosphate dehydrogenase (EC 1.1.1.49). Unlike FDH, these three genes (reactions) function across subcellular compartments at distantly located positions within the metabolic network and are not obviously associated with formic acid biosynthesis or C1 metabolism.

A predicted increase in flux to formic acid is achieved through nonintuitive interactions between *alt2*, *fum1*, and *zwf1* (Figure 1). Although the protein encoded by *FUM1* is both cytoplasmic and mitochondrial (STEIN *et al.* 1994), the model predicted several effects specifically related to its mitochondrial function: (i) decoupling of the respiratory chain resulting in (ii) decreased flux into the key TCA cycle intermediate alpha-ketoglutarate

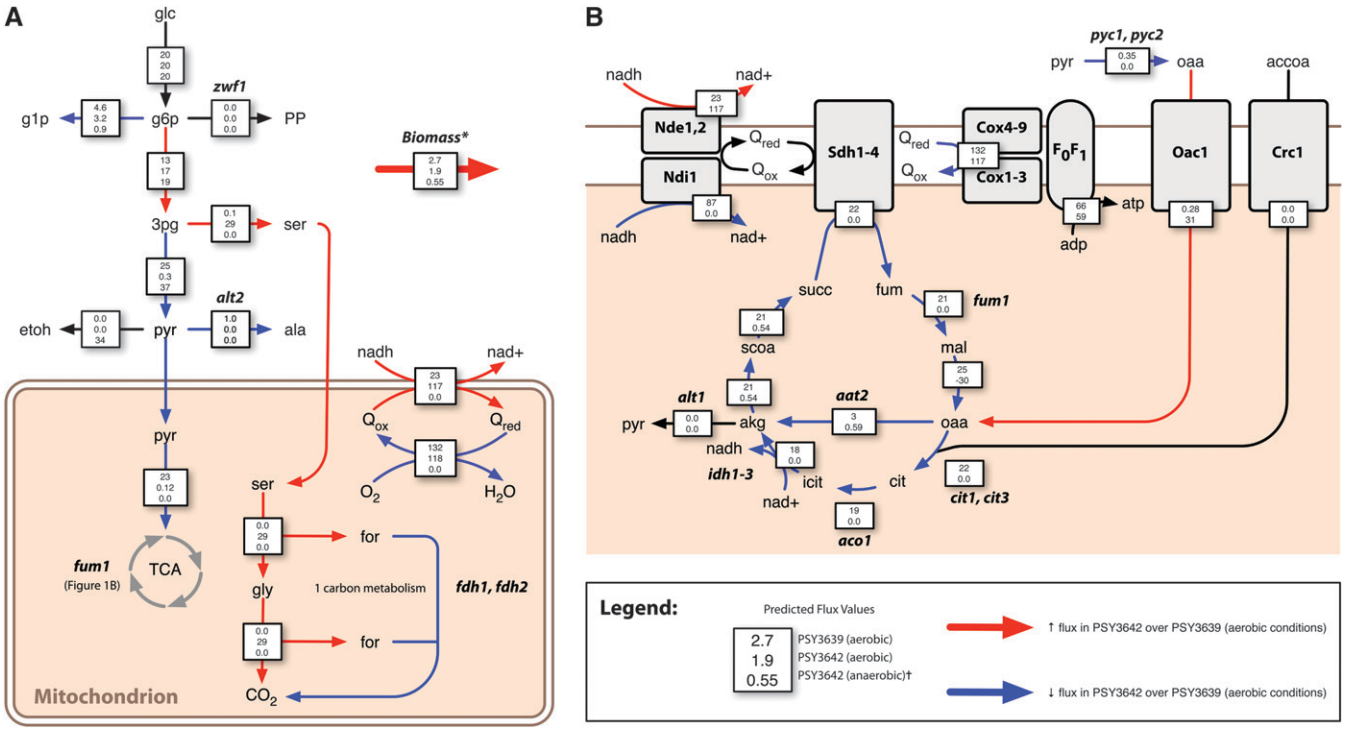

Figure 1.—Constraint-based modeling predicts mutations that redirect flux through serine/glycine biosynthesis and C1 metabolism, leading to increased aerobic formic acid secretion. Arrows denote key cytoplasmic (A) and mitochondrial (B) reactions for which predicted flux is higher (red) or lower (blue) in PSY3642 compared to PSY3639 (see text for details). Boxes superimposed over arrows contain flux values for three simulated conditions: (i) PSY3639 (aerobic), (ii) PSY3642 (aerobic), and (iii) PSY3642 (anaerobic) (†, anaerobic flux values, given in A only). Flux values are relative to a constant glucose uptake rate of 20 mmol gDW^{-1} hr^{-1}. See Table S2 for a complete list of predicted fluxes and metabolites required for growth (*, the biomass equation, given in Table S2). Abbreviations (not provided in the text): glc, glucose; g1p, glucose-1-phosphate; g6p, glucose-6-phosphate; ser, serine; etoh, ethanol; pyr, pyruvate; ala, alanine; gly, glycine; for, formate; nad, nicotinamide adenine dinucleotide; Q, quinone; accoa, acetyl-CoA; cit, citrate; isocit, isocitrate; succ, succinate; fum, fumarate; and mal, malate.

(AKG) and (iii) increased flux into 3-phosphoglycerate (3PG). Flux through PGDH compensates for loss of *FUM1* by balancing 3PG and generating the cytoplasmic AKG—via phosphoserine transaminase (PST) (EC 2.6.1.52) that is necessary for growth. PST catalyzes the transamination of 3-phosphonooxypyruvate, using glutamate as a cofactor, which is balanced by eliminating the competitive reaction associated with *ALT2*. Removing *ZWF1* eliminates direct flux to the pentose phosphate pathway, thereby increasing flux into 3PG, which is balanced by serine/glycine biosynthesis, leading to the complete oxidation of glucose into formic acid, carbon dioxide, and biomass. In the absence of *FDH1* and *FDH2*, intracellular formic acid is balanced by secretion into the media.

Consistent with Equation 1, the FBA model predicts that formic acid secretion is oxygen dependent. Excess reducing equivalents in the form of eight cytoplasmic NADHs are balanced aerobically rather than using an organic substrate as a final electron acceptor. Accordingly, the model predicts increased flux through reactions catalyzed by the external mitochondrial NADH dehydrogenases Nde1 and Nde2 as well as downstream electron transport chain components.

Model validation confirms that elevated formic acid secretion requires aerobic respiration: Results comparing formic acid secretion in PSY3639 and PSY3642 revealed broad qualitative agreement with two important model predictions: (i) mutations in *alt2*, *fum1*, and *zwf1* interacted in a combinatorial manner to enhance formic acid production and (ii) this enhancement was oxygen dependent.

The rate of formic acid secretion measured during log-phase growth was significantly (3-fold) higher in PSY3642 compared to PSY3639 ($P < 0.01$) and this change was dependent on aerobic growth conditions (Figure 2A). Furthermore, formic acid secretion increased nonlinearly with enzyme loss, indicating a cumulative increase in formic acid production that resulted from eliminating combinatorial interactions between the deleted enzymes (Figure 2B). Because FBA models flux at quasi-steady state, derived predictions are generally applicable only during log-phase growth. However, comparisons of PSY3642 and PSY3639 made after saturation (>30 hr of continuous growth) revealed a striking 16.5-fold increase in extracellular formic acid concentration (Figure 2C). Consistent with model predictions, this difference in total formic acid secre-

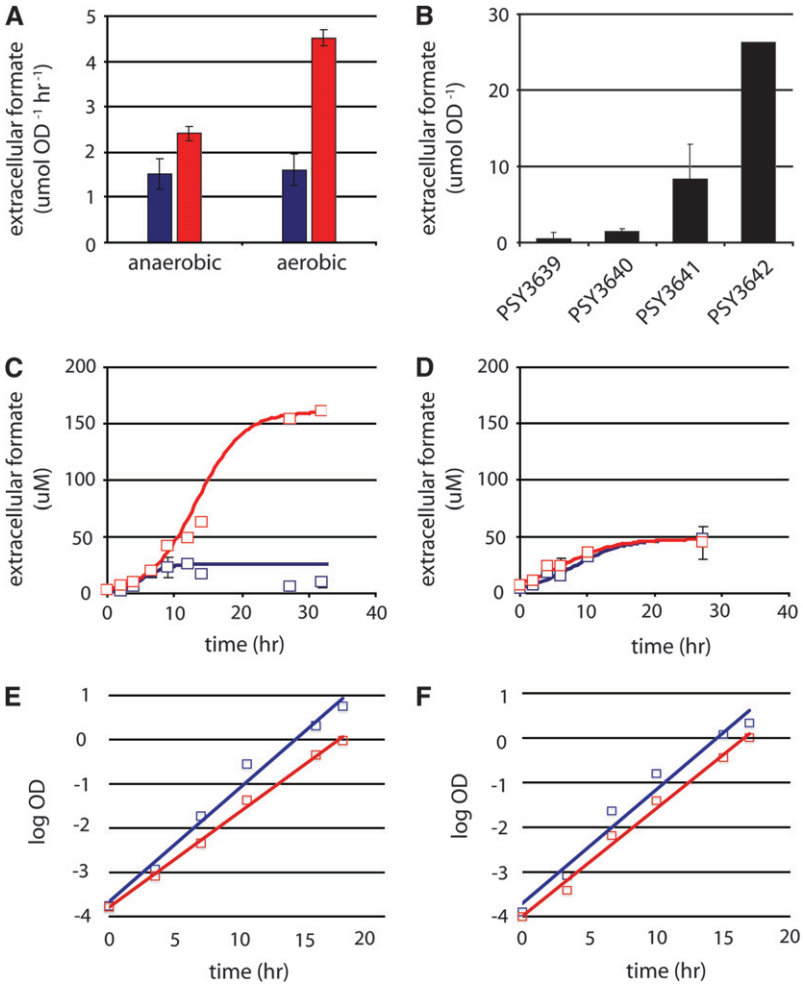

FIGURE 2.—Experimental validation of model predictions. (A) Formic acid secretion rates under aerobic and anaerobic growth conditions; (B) total extracellular formic acid production for several strains, including PSY3639 (blue) and PSY3642 (red), grown aerobically (C) and anaerobically (D). Growth rates are given for PSY3639 and PSY3642 grown aerobically (E) and anaerobically (F). Genotypes for strains in B are listed in Table 2. Fit curves in C–F were calculated using logistic regression. Data represent the average of three biological replicates ± SD. A paired two-tailed *t*-test was used to test for statistical significance in A.

tion was observed only under aerobic growth conditions (Figure 2D).

Under aerobic conditions, the model predicted a slight growth disadvantage in PSY3642 attributed to diversion of carbon flux away from biomass into formic acid synthesis (Figure 1A) whereas under anaerobic conditions the predicted growth rates for the two strains were equivalent (data not shown). Consistent with these predictions, under aerobic conditions we observed a substantial growth defect (0.17 hr^{-1} *vs.* 0.26 hr^{-1}) (Figure 2E). Under anaerobic conditions, the two strains had comparable growth rates (0.23 hr^{-1} *vs.* 0.24 hr^{-1}) (Figure 2F). One simple explanation for the exacerbated growth defect observed in PSY3642 was toxicity. However, the addition of high concentrations of extracellular formic acid up to 100 mM was well tolerated and did not affect relative rates of growth or cell lysis in either strain (data not shown).

Engineering endogenous C1 metabolism induces the retrograde response: To gain insight into potential transcriptional mechanisms underlying increases in formic acid secretion, we performed gene expression analysis comparing PSY3639 and PSY3642 by competitive hybridization to whole-genome cDNA microarrays (see MATERIALS AND METHODS). Bioinformatics analysis of these data implicated specific transcriptional responses resulting from manipulating C1 metabolism for formic acid production. An initial assessment of genes with the highest differential expression (some as high as 56-fold) revealed a varied transcriptional response involving disparate biological processes, including glucose repression (*GCR1* and *RGR1*), mitochondrial function (*ATP15*, *FMT1*, *RPM2*, and *QCR10*), telomere maintenance (*ESC8*, *RSC58*, and *SIR3*), and C1 metabolism (*ADE4*, *ATP2*, *ATP7*, *FOL1*, *FMT1*, and *POR1*) (Table 3). Significant gene ontology enrichments were identified for enzymes primarily involved in mitochondrial-associated reactions ($P = 0.01$), including TCA metabolic processes ($P = 0.02$) and oxidative phosphorylation ($P = 0.005$). These results are generally consistent with glycine-induced transcriptional changes observed for C1 metabolic enzymes (GELLING *et al.* 2004).

To identify similar patterns of expression in other mutant backgrounds, we compared the gene expression profile of PSY3642 with the compendium generated by HUGHES *et al.* (2006). Using hierarchical clustering of these data, we identified patterns of expression that

TABLE 3

Differentially expressed genes in PSY3642

Gene	ORF	Function	Fold change
ADE4	YMR300C	Phosphoribosylpyrophosphate amidotransferase	−56.6
ATP15	YPL271W	ATP synthase epsilon subunit	−12.7
FMT1	YBL013W	Formyl–methionyl–tRNA transformylase	−8.5
ESC8	YOL017W	Telomeric and mating-type locus silencing	−8.2
QCR10	YHR001W-A	Ubiqunol–cytochrome c oxidoreductase complex	−7.7
POR1	YNL055C	Outer mitochondrial membrane porin	−4.1
ATP7	YKL016C	ATP synthase D subunit	−3.3
ATP2	YJR121W	F(1)F(0)-ATPase complex β-subunit	−2.2
SER3	YER081W	Catalyzes the first step in serine biosynthesis	1.8
ADH3	YMR083W	Alcohol dehydrogenase isoenzyme	1.9
RTG1	YOL067C	Interorganelle communication	4.7
CRC1	YOR100C	Mitochondrial carnitine carrier	4.8
FOL1	YNL256W	Folic acid synthesis	5.7
IDH1	YNL037C	Mitochondrial isocitrate dehydrogenase	5.8
RGR1	YLR071C	Transcriptional regulation of diverse genes	6.6
IDH2	YOR136W	NAD+-dependent isocitrate dehydrogenase	6.6
OAC1	YKL120W	Mitochondrial oxaloacetate carrier	7.0
SIR3	YLR442C	Silencing at HML, HMR, and telomeres	9.9
GCR1	YPL075W	Positive regulator of the enolase	11.7
RSC58	YLR033W	Chromatin remodeling complex subunit	12.1
RPM2	YML091C	Mitochondrial precursor tRNAs	44.7

were similar to the profile observed in PSY3642 (Figure 3A). Each of these profiles was associated with a particular conditional experiment. We chose to limit our analysis to gene expression profiles generated from gene deletions. PSY3642-similar expression patterns were associated with specific gene mutations affecting chromatin function and general transcriptional regulation, MAP kinase signal transduction (*swi6*, *sst2*, *dig1*, and *dig2*), mitochondrial function (*rip1*, *qcr2*, *kim4*, etc.), and cell wall (*gas1*, *anp1*, *fks1*, etc.) and ergosterol biosynthesis (*erg2* and *erg3*). Interestingly, single deletions in *SSN6*, *RPD3*, or *TUP1*—components of a well-characterized transcriptional silencing complex—resulted in the differential expression of >180 genes (Smith and Johnson 2000; Green and Johnson 2004), many of which were also differentially expressed in PSY3642. Motif enrichments in the promoters of upregulated genes implicated transcription factors associated with several biological processes (Figure 3B). Included in this set were Rtg1 and Rtg3, two transcription factors that mediate mitochondria-to-nucleus retrograde signaling in response to severe mitochondrial dysfunction.

Retrograde signaling is typically associated with the petite phenotype caused by loss of mitochondrial DNA (ρ^0) (Butow and Avadhani 2004). Cells sense mitochondrial dysfunction and implement systemic changes in gene expression to compensate for mitochondria-associated metabolic deficiencies (Liu and Butow 2006). In ρ^0 yeast, Rtg1-mediated retrograde signaling is exclusively post-translational: phosphorylated Rtg1 translocates to the nucleus without any change in the abundance of *RTG1* transcript itself; however, in PSY3642 expression of *RTG1* is significantly upregulated (Table 3). This suggests an alternative (transcriptional) mode of Rtg1-mediated retrograde signaling that is absent in ρ^0 yeast.

Using mitochondria-specific vital stains we confirmed the mitochondrial defect implied by induced expression of *RTG1* and transcriptional induction of retrograde responsive genes. Whereas PSY3639 resembled wild-type yeast with regard to mitochondrial abundance, morphology, and membrane potential, analysis of PSY3642 revealed a heterogeneous population of cells that were depleted in functional mitochondria (Figure 4). Microscopic analysis revealed a dramatic reduction in both the total number of mitochondria and their associated respiratory capacity (compare Figure 4, A and C, to Figure 4, B and D). This effect was primarily evident in PSY3642, with strains PSY3640 and PSY3641 resembling the parent strain PSY3639 (Figure S1). These data, along with experiments that show elevated formic acid secretion exclusively under oxygenated growth conditions (Figure 2), indicate that mitochondrial function and respiratory capacity are severely diminished but not completely abolished in PSY3642.

ρ^0 yeast upregulate several genes to provide stoichiometric amounts of oxaloacetate and acetyl-CoA to drive the TCA cycle in the presence of respiratory deficiency (Epstein *et al.* 2001). Several of these genes are also upregulated in PSY3642, including *PYC1*, *OAC1*, and *CRC1*, as well as the NAD-dependent TCA cycle enzymes

B

Motif	Factors	Function
TTTCTTT	Azf1	Mitochondrial transcription
AGGA	Cat8, Sip4	Glucose catabolism
CTTC	Gcr1	
TTTCT	Mig1-3	
GGAA	Rgt1	
ATAA	Dal80	Nitrogen metabolism
TCTTT	Dal81, 82	
TATAT	Hap1	Respiratory gene expression
ACCA	Hap2-5	
TCTTG	Rox1	
TATA	Ecm22, Upc2	Sterol synthesis
AAGA	Mot3	
CTTG	Abf1	Chromatin organization
ATAC	Rap1	
TACC	Rep1	
GGTA	Rtg1, 3	Retrograde signaling

FIGURE 3.—Expression analysis of PSY3642. (A) Hierarchical clustering of PSY3642 and other mutant strain expression profiles are represented as a clustering diagram (dendogram). For clarity, only a portion (approximately one-third) of the complete dendogram is shown. The cluster subtrees are ordered and displayed nonrandomly such that similar expression profiles appear closer together. Labels for several functional categories reflect the tendency for strains with comparable genetic deficiencies to exhibit similar patterns of gene expression (HUGHES *et al.* 2006). PSY3642 clusters close to strains with mutations affecting chromatin function, MAP kinase signaling, and mitochondrial function (see text for details). (B) DNA-binding motifs ($P < 10^{-10}$) within the promoters of activated genes in PSY3642 are represented as sequence logos (left column) along with cognate transcription factors (middle column) and identified regulatory roles (right column).

IDH1 and *IDH2* (Table 3). As the FBA model predicted very little flux through the TCA cycle, a retrograde responsive increase in flux through these reactions represents an unanticipated (and unforeseeable) adaptation to manipulating C1 metabolism. We constructed an *rtg1* mutation in the PSY3642 genetic background (PSY3650) and observed a 25% increase in formic acid secretion (Table 4).

In the presence of severe respiratory deficiency, increased TCA cycle flux would be coupled to increased flux through NAD-dependent reactions (for example, through increased expression of *IDH1* and *IDH2*). As a result the cell would require some biochemical mechanism to regenerate NAD and maintain redox homeostasis. ρ^0 yeast upregulate the expression of glycerol-3-phosphate and alcohol dehydrogenase enzymes (Gpd2 and Adh1-7) as part of the retrograde response. These pathways reoxidize NADH in the absence of competent oxidative capacity (EPSTEIN *et al.* 2001). In PSY3642 there is no significant change in expression of *GPD2*, *ADH1*, or *ADH4–7*. *ADH3*, a mitochondrial ethanol-acetaldehyde redox shuttle (BAKKER *et al.* 2000), is induced twofold; however, we observed no detectable difference in ethanol production between PSY3642 and PSY3639 (Table 4). To test the hypothesis that flux through NAD-dependent reactions increases in PSY3642 we measured intracellular NADH/NAD ratios directly (see MATERIALS AND METHODS). We observed a significant increase in intracellular NADH relative to NAD, which was eliminated in *rtg1* mutants (Figure 5). Together, these results support the hypothesis of an Rtg1-mediated increase in flux to the TCA cycle, which increases the NADH/NAD ratio and diverts organic substrate away from C1 metabolism and formic acid biosynthesis.

Increased flux to formic acid is modulated by coordinated expression of C1 pathway enzymes: According to our pathway analysis of C1 metabolism, the enzymes associated with Equation 1 are both necessary and sufficient to catalyze the full oxidation of glucose into formic acid given proper regulatory constraints that serve to channel flux through this pathway. Transcriptional coregulation of the upstream portion of Equation 1 (glycolysis) is well characterized. By combining pathway analysis and transcriptional data, we tested the hypothesis that downstream reactions occurring after the glycolytic branch point PGDH are also subject to coregulation. We sought to identify endogenous transcriptional programs responsible for increased C1 metabolic flux in PSY3642.

A closer look at relative mRNA abundance for enzymes involved in formic acid biosynthesis revealed an interesting pattern of endogenous differential expression (Figure 6B). Relative to the branch point isozyme Ser3 (PGDH), differential expression of downstream enzymes is correlated to their relative position in

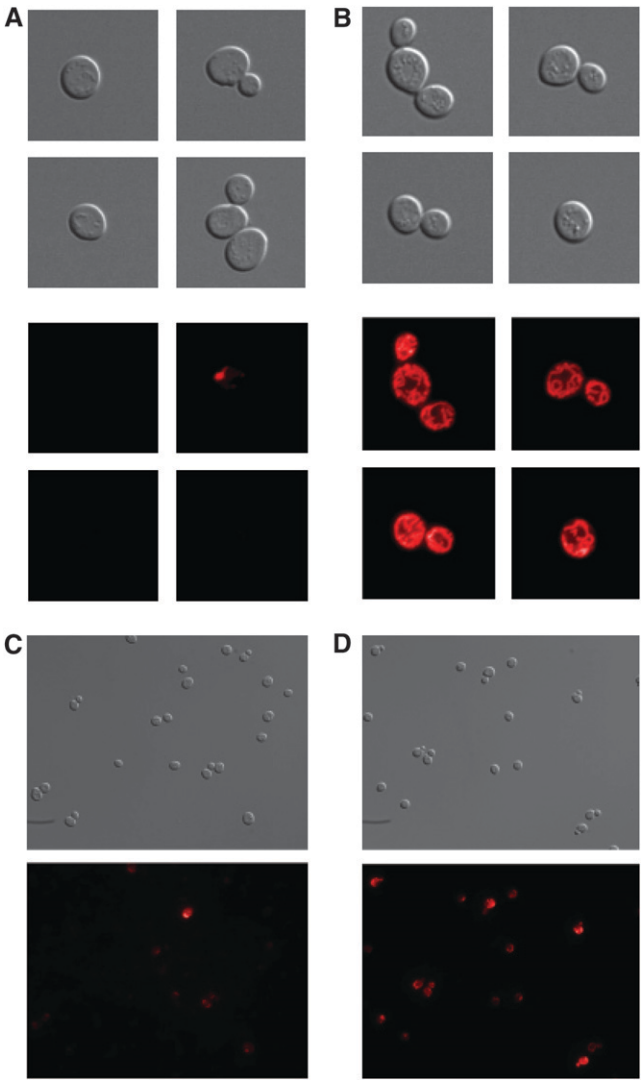

FIGURE 4.—Phenotypic analysis of PSY3642 reveals mitochondrial dysfunction. Total mitochondria were labeled in PSY3642 (A) and PSY3639 (B) and single cells were imaged at 100× magnification with DIC (top panels) and epifluorescence (bottom panels). Oxidation of Mitotracker CM-H_2XRos was measured to indicate respiratory capacity in PSY3642 (C) and PSY3639 (D). Cells were imaged at 40× magnification with DIC (top panels) and epifluorescence (bottom panels). Exposure times were 40 msec in all cases.

the pathway, with the lowest expression change associated with the terminal enzyme Mis1. Linear regression indicates that 52% of the variance in differential expression of C1-associated enzymes is explained simply by their relative topological position in the reaction pathway ($P = 0.02$). Interestingly, this pattern of differential expression implicates a recognized mechanism of endogenous metabolic control termed multisite modulation, where coordinated expression of several enzymes modulates flux through entire metabolic pathways (FELL 1997). This provides experimental evidence that C1 enzymes constitute a module of pathway function in PSY3642.

TABLE 4

Quantification of Rtg1-mediated formic acid secretion

Strain	Formic acid (mM)[a]	Ethanol (mM)[a]
PSY3639	0.01 ± 0.005	155 ± 19
PSY3642	0.16 ± 0.004	178 ± 14
PSY3650	0.2 ± 0.01	NA

[a] Data are given as the average of three biological replicates ± SD.

The transcriptional data we obtained suggested that increased expression of Ser3 was causally associated with increased flux to formic acid (Table 3). Generally, overexpressing branch point enzymes rarely affects their associated flux to any significant degree. This is due, in part, to feedback inhibition by downstream metabolites (FELL 1997). Indeed, PGDH is allosterically inhibited by serine and, as a consequence, it has very low flux control in mammalian tissue (; FELL and SNELL 1988; BELL *et al.* 2004; THOMPSON *et al.* 2005). To test the hypothesis that PGDH may control formic acid synthesis in PSY3642, we generated a plasmid for inducible overexpression of the catalytic domain of *E. coli* SerA (pRS410a), a well-characterized functional homolog of yeast Ser3. Expression levels of the fusion protein were not affected by strain-specific genetic backgrounds or transcriptional induction (Figure 6C). Consistent with previous experiments in mammalian tissues, SerA had no effect on flux to formic acid in PSY3639; however, SerA expression in PSY3642 resulted in an 86% increase in extracellular formic acid concentration (Figure 6D). This result is consistent with endogenous induction of Ser3 in PSY3642 and suggests that PGDH has a positive flux control coefficient in this strain.

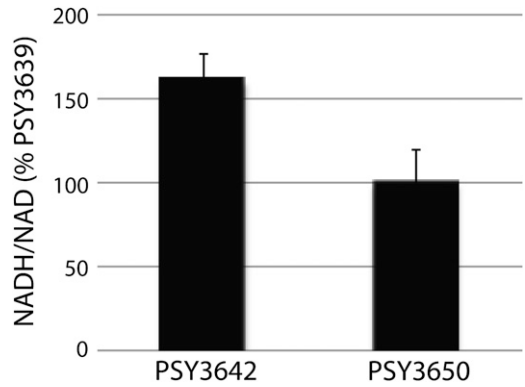

FIGURE 5.—Increase in NADH/NAD in PSY3642 NADH/NAD ratios for PSY3642 and PSY3650 is given as percentage of PSY3639. Data represent the average of four biological replicates ± SD. Compared to that in PSY3639, NADH accumulated significantly in PSY3642 ($P = 0.001$) but not in PSY3650 ($P = 0.46$). Statistical significance was assessed by testing the null hypothesis $m = 100\%$ *vs.* the alternative $m > 100\%$, assuming normally distributed sample data.

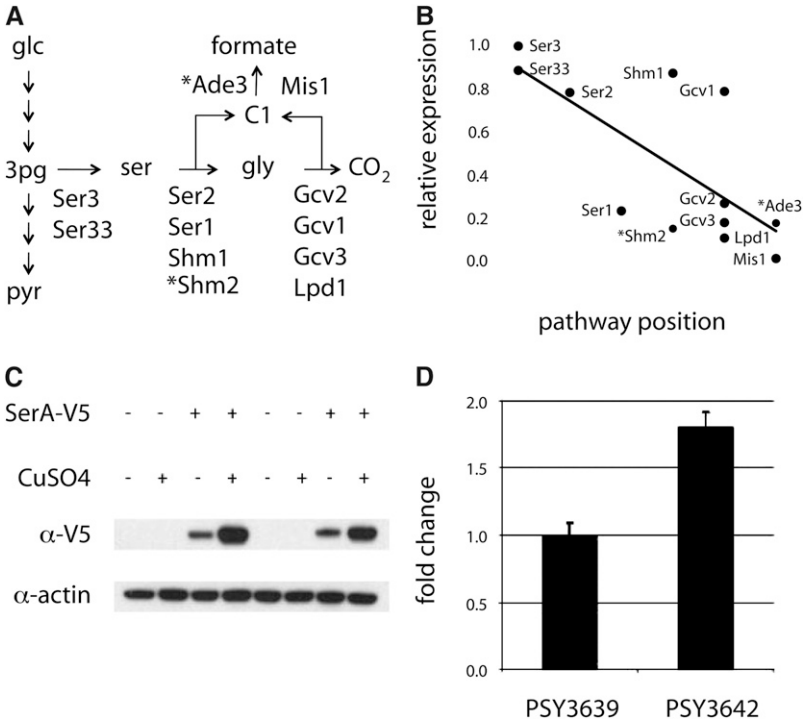

FIGURE 6.—Flux to formic acid is controlled by PGDH and the coordinated expression of all pathway enzymes. (A) The subnetwork of serine–glycine–formate biosynthesis with reaction arrows that represent composites of several biochemical interconversions labeled with relevant enzymes. The cytoplasmic enzymes involved in converting serine into formic acid (Shm2 and Ade3) are denoted with asterisks. (B) Differential expression of enzymes in A were normalized to Ser3 and plotted according to their pathway position. Multisite modulation for enzymes in the formic acid biosynthetic pathway is indicated by linear regression (solid line, $R^2 = 0.52$) and corrected Spearman's ranked order correlation ($\rho = -0.72$, $P = 0.02$). (C) Levels of the SerA fusion protein (relative to actin) were unaffected by genetic background and induction conditions. (D) Expressing SerA in PSY3642 caused a significant increase in formic acid secretion under inducing conditions. Each transformed strain was normalized to the empty vector control plasmid pRS410a. Data in D represent the average of three biological replicates ± SD. We assessed statistical significance using a paired two-tailed *t*-test ($P = 0.002$).

DISCUSSION

Our goal in this work was to test an FBA-based strategy for engineering C1 metabolism in yeast to increase endogenous formic acid production and describe cellular mechanisms responsible for regulating this important metabolic pathway. FBA and gene knockout simulations identified a nonintuitive combination of genes (*ALT2*, *FUM1*, and *ZWF1*), which individually had no obvious role in formic acid biosynthesis (Figure 1). On the basis of the model predictions, we constructed the quintuple knockout *alt2 fdh1 fdh2 fum1 zwf1* and showed significant oxygen-dependent formic acid secretion in the engineered strain, during both log-phase (Figure 2A) and stationary-phase growth (Figure 2, C and D). Further, maximum formic acid secretion required all five enzyme deletions predicted by the model (Figure 2B). Although formic acid is an essential intracellular metabolite, it is not secreted in detectable levels in wild-type yeast (McNeil *et al.* 1996; Blank *et al.* 2005). Thus, our results demonstrate the successful application of an FBA-based strategy for microbial production of formic acid under aerobic growth conditions. More generally, these data support the predictive potential for this approach in deriving strategies aimed at engineering nonfermentative metabolic pathways that integrate across subcellular compartments in eukaryotic microbes.

To gain insights into the regulatory events that result from manipulating formic acid biosynthesis, we supplemented model predictions and validation experiments with gene expression and phenotypic analyses. From these data we identified (i) a significant transcriptional response involving multiple cellular processes (Table 3 and Figure 3); (ii) activation of retrograde signaling, mitochondrial dysfunction, and diminished respiratory capacity (Table 4 and Figures 4 and 5); and (iii) transcriptional regulatory events that lead to the coordinated expression of enzymes involved in C1 metabolism (Figure 6). Upon close inspection, these data indicate specific mechanisms of metabolic regulation that result from unanticipated adaptive responses to manipulating C1 metabolic flux.

Several lines of evidence strongly suggest activation of the retrograde response in PSY3642 cells. In terms of global gene expression pattern, PSY3642 is most similar to strains with mutations in genes that are directly involved in retrograde signaling (Figure 3A). These include Rpd3, Ssn6, and Tup1, a well-characterized corepressor complex (Malave and Dent 2006), and Yat2, a carnitine acetyl-CoA transferase involved in transporting activated acetate into respiratory deficient mitochondria (Epstein *et al.* 2001; Swiegers *et al.* 2001; Liu and Butow 2006). Interestingly, Yat2 was identified in our original *in silico* knockout screen for enzymes that affect C1 metabolic flux (Table 1).

In petite cells Ssn6–Tup1 is converted from a transcriptional corepressor complex into a coactivator, which upregulates gene expression through direct interaction with Rtg3 (Conlan *et al.* 1999), one of three transcription factors primarily responsible for retrograde responsive gene activation in yeast (Rothermel *et al.* 1997). DNA binding motifs for Rtg1 and Rtg3 are overrepresented in the promoters of activated genes in PSY3642 (Figure 3D) while *RTG1* expression itself is increased almost fivefold (Table 3). These results strongly implicate

retrograde regulatory transcription factors as specific modulators of gene activation and metabolic activity in PSY3642. Consistent with this hypothesis are data showing Rtg1-dependent NADH accumulation and limitations in formic acid biosynthesis (Figure 5 and Table 4).

While *zwf1* mutants have no mitochondrial defects (Blank *et al.* 2005), Wu and Tzagoloff (1987) speculated that the petite-like phenotype of *fum1* mutants is caused by decreased concentrations of intramitochondrial amino acids, which limits the production of respiratory chain components. However, loss of Fum1 alone does not account for retrograde signaling in PSY3642, as transcriptional changes in *fum1* single mutants are limited; only ~20 genes are affected, none of which encode typical retrograde responsive TCA cycle enzymes (McCammon *et al.* 2003). Furthermore, although Gelling *et al.* (2004) showed that C1 metabolic flux changes significantly affect the expression status of respiratory chain components, mitochondrial deficiency and retrograde signaling were not reported as a consequence. From these results we conclude that enzyme deletions predicted by our model cause systemic metabolic changes that modulate C1 flux and activate retrograde signaling in PSY3642. Specifically, *alt2*-associated loss of cytoplasmic alanine transaminase activity—either alone or in combination with *fum1* or *zwf1* mutations—may significantly diminish aminogenic capacity leading to full activation of the retrograde response. Alternatively, retrograde signaling may result from reduced intracellular concentrations of specific retrograde inhibitors such as glutamate, glutamine, or ammonia (Crespo *et al.* 2002; Tate and Cooper 2003; Butow and Avadhani 2004; Dilova *et al.* 2004).

Multisite modulation is an important mechanism of metabolic control, where changes in pathway flux result from the coordinated expression of multiple pathway enzymes in relative proportion to their distance from the main pathway branch point (Thomas and Fell 1996; Fell 1997). Accumulating evidence obtained in yeast (Niederberger *et al.* 1992), mammals (Brownie and Pedersen 1986; Waterman and Simpson 1989; Hillgartner *et al.* 1995; Vogt *et al.* 2002; Werle *et al.* 2005), and plants (Quick *et al.* 1991; Stitt *et al.* 1991; Anterola *et al.* 1999) suggests that multisite modulation may be a general design principle employed by cells to regulate metabolic flux *in vivo* (Wildermuth 2000). Indeed, using formal pathway analysis, we identified a module of pathway function corresponding to downstream reactions in C1 metabolism (Equation 1) and observed a pattern of differential expression in PSY3642 that strongly suggested multisite modulation of enzymes in this pathway (Figure 6B).

A predominant challenge in constraint-based analysis of metabolic networks involves discovering and incorporating relevant cellular regulatory processes (Price *et al.* 2003; Stelling and Gilles 2004). Because regulatory events are conditional and often characterized by their dynamic nature, they are difficult to predict under the assumptions of conventional FBA (Jamshidi and Palsson 2008). Without the benefit of complete knowledge of gene regulation it is useful to combine systems-level modeling with experimental data generated *post hoc* for the purposes of design and discovery in complex metabolic systems. By combining formal pathway analysis, FBA, and experimentation, we were able to identify and exploit specific modes of endogenous regulation to increase C1 metabolic flux and engineer a formic acid-producing strain of yeast.

We thank Christina Agapakis and Jake Wintermute for comments on the manuscript. This work was supported in part by a National Institutes of Health (NIH) training grant to C.J.K., by an NIH Cell and Developmental Biology training grant (GM07226) to P.M.B., and in part by a grant from the Harvard University Center for the Environment.

LITERATURE CITED

Alper, H., J. Moxley, E. Nevoigt, G. R. Fink and G. Stephanopoulos, 2006 Engineering yeast transcriptional machinery for improved ethanol tolerance and production. Science **314:** 1565–1568.

Anterola, A. M., H. van Rensburg, P. S. van Heerden, L. B. Davin and N. G. Lewis, 1999 Multi-site modulation of flux during monolignol formation in loblolly pine (*Pinus taeda*). Biochem. Biophys. Res. Commun. **261:** 652–657.

Bakker, B. M., C. Bro, P. Kotter, M. A. H. Luttik, J. P. van Dijken *et al.*, 2000 The mitochondrial alcohol dehydrogenase Adh3p is involved in a redox shuttle in *Saccharomyces cerevisiae*. J. Bacteriol. **182:** 4730–4737.

Becker, S. A., and B. O. Palsson, 2008 Context-specific metabolic networks are consistent with experiments. PLoS Comput. Biol. **4:** e1000082.

Bell, J. K., G. A. Grant and L. J. Banaszak, 2004 Multiconformational states in phophoglycerate dehydrogenase. Biochemistry **43:** 3450–3458.

Birkmann, A., F. Zinoni, G. Sawers and A. Böck, 1987 Factors affecting transcriptional regulation of the formate-hydrogen-lyase pathway of Escherichia coli. Arch. Microbiol. **148:** 44–51.

Blank, L. M., L. Kuepfer and U. Sauer, 2005 Large-scale ^{13}C-flux analysis reveals mechanistic principles of metabolic network robustness to null mutations in yeast. Genome Biol. **6:** R49.

Bro, C., B. Regenberg, J. Forster and J. Nielsen, 2006 In silico aided metabolic engineering of *Saccharomyces cerevisiae* for improved bioethanol production. Metab. Eng. **8:** 102–111.

Brownie, A. C., and R. C. Pedersen, 1986 Control of aldosterone secretion by pituitary hormones. J. Hypertens. Suppl. **4:** S72–S75.

Burgard, A. P., P. Pharka and C. D. Maranas, 2003 Optknock: a bilevel programming framework for identifying gene knockout strategies for microbial strain optimization. Biotechnol. Bioeng. **84:** 647–657.

Butow, R. A., and N. G. Avadhani, 2004 Mitochondrial signaling: the retrograde response. Mol. Cell **14:** 1–15.

Canelas, A. B., W. M. van Gulik and J. J. Heijnen, 2008 Determination of the cytosolic free NAD/NADH ratio in Saccharomyces cerevisiae under steady-state and highly dynamic conditions. Biotechnol. Bioeng. **100:** 734–743.

Christensen, K. E., and R. E. MacKenzie, 2006 Mitochondrial one-carbon metabolism is adapted to the specific needs of yeast, plants and mammals. BioEssays **28:** 595–605.

Conlan, S. R., N. Gounalaki, P. Hatis and D. Tzamarias, 1999 The Tup1-Cyc8 protein complex can shift from a transcriptional co-repressor to a transcriptional co-activator. J. Biol. Chem. **1:** 205–210.

Cordier, H., F. Mendes, I. Vasconcelos and J. M. Francois, 2007 A metabolic and genomic study of engineered *Saccharomyces cerevisiae* strains for high glycerol production. Metab. Eng. **9:** 364–378.

Crespo, J. L., T. Powers, B. Fowler and M. N. Hall, 2002 The TOR-controlled transcription activators *GLN3*, *RTG1*, and *RTG3*, are regulated in response to intracellular levels of glutamine. Proc. Natl. Acad. Sci. USA **99:** 6784–6789.

Dilova, I., S. Aronova, J. C.-Y. Chen and T. Powers, 2004 Tor signaling and nutrient-based signals converge on Mks1p phosphorylation to regulate expression of Rtg1p-Rtg3p-dependent target genes. J. Biol. Chem. **45:** 46527–46535.

Di Pierro, D., B. Tavazzi, C. F. Perno, M. Bartolini, E. Balestra *et al.*, 1995 An ion-pairing high-performance liquid chromatographic method for the direct simultaneous determination of nucleotides, deoxynucleotides, nicotinic coenzymes, oxypurines, nucleosides, and bases in perchloric acid cell extracts. Anal. Biochem. **231:** 407–412.

Duarte, N. C., M. J. Herrgård and B. O. Palsson, 2004 Reconstruction and validation of Saccharomyces cerevisiae *i*ND750, a fully compartmentalized genome-scale metabolic model. Genome Res. **14:** 1298–1309.

Edwards, J. S., and B. O. Palsson, 2000 The *Eschericia coli* MG1655 in silico metabolic genotype: its definition, characteristics, and capabilities. Proc. Natl. Acad. Sci. USA **97:** 5528–5533.

Epstein, C. B., J. A. Waddle, W. Hale, 4th, V. Dave, J. Thornton *et al.*, 2001 Genome-wide responses to mitochondrial dysfunction. Mol. Biol. Cell **12:** 297–308.

Fell, D. A., 1997 *Frontiers in Metabolism: Understanding the Control of Metabolism.* Portland Press, London.

Fell, D. A., and K. Snell, 1988 Control analysis of mammalian serine biosynthesis. Feedback inhibition on the final step. Biochem. J. **256:** 97–101.

Forster, J., I. Famili, B. Palsson and J. Nielsen, 2003 Large-scale evaluation of *in silico* gene knockouts in *Saccharomyces cerevisiae.* OMICS **7:** 193–202.

Fu, T. F., J. P. Rife and V. Schirch, 2001 The role of serine hydroxymethyltransferase isozymes in one-carbon metabolism in MCF-7 cells as determined by ^{13}C NMR. Arch. Biochem. Biophys. **393:** 42–50.

Geertman, J. M., A. J. van Maris, J. P. van Dijken and J. T. Pronk, 2006 Physiological and genetic engineering of cytosolic redox metabolism in *Saccharomyces cerevisiae* for improved glycerol production. Metab. Eng. **8:** 532–542.

Gelling, C. L., M. D. Piper, S. P. Hong, G. D. Kornfeld and I. W. Dawes, 2004 Identification of a novel one-carbon metabolism regulon in *Saccharomyces cerevisiae.* J. Biol. Chem. **279:** 7072–7081.

Green, S. R., and A. D. Johnson, 2004 Promoter-dependent roles for the Srb10 cyclin-dependent kinase and the Hda1 deacetylase in Tup1-mediated repression in *Saccharomyces cerevisiae.* Mol. Biol. Cell **15:** 4191–4202.

Guldener, U., S. Heck, T. Fiedler, J. Beinhauer and J. H. Hegemann, 1996 A new efficient gene disruption cassette for repeated use in budding yeast. Nucleic Acids Res. **24:** 2519–2524.

Hefetz, A., and M. S. Blum, 1978 Biosynthesis of formic acid by the poison glands of formicine ants. Science **201:** 454–455.

Herrero, O., D. Ramon and M. Orejas, 2008 Engineering the *Saccharomyces cerevisiae* isoprenoid pathway for de novo production of aromatic monoterpenes in wine. Metab. Eng. **10:** 78–86.

Hillgartner, F. B., L. M. Salati and A. G. Goodridge, 1995 Physiological and molecular mechanisms involved in nutritional regulation of fatty acid synthesis. Physiol. Rev. **75:** 47–76.

Hjersted, J. L., M. A. Henson and R. Mahadevan, 2007 Genome-scale analysis of *Saccharomyces cerevisiae* metabolism and ethanol production in fed-batch culture. Biotechnol. Bioeng. **97:** 1190–1204.

Hughes, T. R., M. J. Marton, A. R. Jones, C. J. Roberts, R. Stoughton *et al.*, 2006 Functional discovery via a compendium of expression profiles. Cell **102:** 109–126.

Ishida, N., S. Saltoh, T. Ohnishi, K. Tokuhiro, E. Nagamori *et al.*, 2006 Metabolic engineering of *Saccharomyces cerevisiae* for efficient production of pure L: -(+)-lactic acid. Appl. Biochem. Biotechnol. **131:** 795–807.

Jamshidi, N., and B. O. Palsson, 2008 Formulating genome-scale kinetic models in the post-genome era. Mol. Syst. Biol. **4:** 171.

Kastanos, E. K., Y. Y. Woldman and D. R. Appling, 1997 Role of mitochondrial and cytoplasmic serine hydroxymethyltransferase isozymes in *de novo* purine synthesis in *Sacharomyces cerevisiae.* Biochemistry **36:** 14956–14964.

Kizer, L., D. J. Pitera, B. F. Pfleger and J. D. Keasling, 2008 Application of functional genomics to pathway optimization for increased isoprenoid production. Appl. Environ. Microbiol. **74:** 3229–3241.

Klamt, S., and J. Stelling, 2002 Combinatorial complexity of pathway analysis in metabolic networks. Mol. Biol. Rep. **29:** 233–236.

Knight, T., 2003 Idempotent vector design for standard assembly of biobricks. In DSpace. MIT Artificial Intelligence Laboratory, MIT Synthetic Biology Working Group. http://hdl.handle.net/1721.1/21168.

Lange, H. C., M. Eman, G. van Zuijlen, D. Visser, J. C. van Dam *et al.*, 2001 Improved rapid sampling for in vivo kinetics of intracellular metabolites in Saccharomyces cerevisiae. Biotechnol. Bioeng. **75:** 406–415.

Lee, J., A. Goel, M. M. Ataii and M. M. Domach, 1997 Supply-side analysis of growth of *Bacillus subtilis* on glucose-citrate medium: feasible network alternatives and yield optimality. Appl. Environ. Microbiol. **63:** 710–718.

Lee, S., C. Phalakornkule, M. M. Domach and I. E. Grossmann, 2000 Recursive MILP model for finding all alternate optima in LP models for metabolic networks. Comp. Chem. Eng. **24:** 711–716.

Leonhartsberger, S., I. Korsa and A. Bock, 2002 The molecular biology of formate metabolism in enterobacteria. J. Mol. Microbiol. Biotechnol. **4:** 269–276.

Liu, Z., and R. A. Butow, 2006 Mitochondrial retrograde signaling. Annu. Rev. Genet. **40:** 159–185.

Ludovico, P., F. Rodrigues, A. Almeida, M. T. Silva, A. Barrientos *et al.*, 2002 Cytochrome c release and mitochondria involvement in programmed cell death induced by acetic acid in *Saccharomyces cerevisiae.* Mol. Cell. Biol. **13:** 2598–2606.

Malave, T. M., and S. Y. Dent, 2006 Transcriptional repression by Tup1-Ssn6. Biochem. Cell Biol. **84:** 437–443.

McCammon, M. T., C. B. Epstein, B. Przybyla-Zawislak, L. McAlister-Henn and R. A. Butow, 2003 Global transcription analysis of Krebs tricarboxylic acid cycle mutants reveals an alternating pattern of gene expression and effects on hypoxic and oxidative genes. Mol. Biol. Cell **14:** 958–972.

McNeil, J. B., A. L. Bognar and R. E. Pearlman, 1996 In vivo analysis of folate coenzymes and their compartmentalization in Saccharomyces cerevisiae. Genetics **142:** 371–381.

Milliken, C. E., and H. D. May, 2007 Sustained generation of electricity by the spore-forming, Gram-positive, *Desulfitobacterium hafniense* strain DCB2. Appl. Microbiol. Biotechnol. **73:** 1180–1189.

Monteiro, P. T., N. Mendes, M. C. Teixeira, S. d'Orey, S. Tenreiro *et al.*, 2008 YEASTRACT-DISCOVERER: new tools to improve the analysis of transcriptional regulatory associations in *Saccharomyces cerevisiae.* Nucleic Acids Res. **36:** D132–D136.

Motter, A. E., N. Glubahce, E. Almass and A. L. Barabasi, 2008 Predicting synthetic rescues in metabolic networks. Mol. Syst. Biol. **4:** 168.

Murtagh, F., 1985 Multidimensional clustering algorithms. Physica-Verlag, Wuerzburg, Germany.

Niederberger, P., R. Prasad, G. Miozzari and H. Kacser, 1992 A strategy for increasing an in vivo flux by genetic manipulations. The tryptophan system of yeast. Biochem. J. **287:** 473–479.

Oh, Y.-K., B. O. Palsson, S. M. Park, C. H. Schilling and R. Mahadevan, 2007 Genome-scale reconstruction of metabolic network in *Bacillus subtillis* based on high-throughput phenotyping and gene essentiality data. J. Biol. Chem. **282:** 28791–28799.

Overkamp, K. M., P. Kötter, R. van der Hoek, S. Schoondermark-Stolk, M. A. Luttik *et al.*, 2002 Functional analysis of structural genes for NAD(+)-dependent formate dehydrogenase in Saccharomyces cerevisiae. Yeast **19:** 509–520.

Papin, J., N. Price, J. Edwards and B. Palsson, 2002 The genome-scale metabolic extreme pathway structure in *Haemophilus influenzae* shows significant network redundancy. J. Theor. Biol. **215:** 67–82.

Peters-Wendisch, P., M. Stolz, H. Etterich, N. Kennerknecht, H. Sahm *et al.*, 2005 Metabolic engineering of *Corynebacterium glutamicum* for L-serine production. Appl. Environ. Microbiol. **71:** 7139–7144.

Phalakornkule, C., S. Lee, T. Zhu, R. Koepsel, M. M. Ataai *et al.*, 2001 A MILP-based flux alternative generation and NMR experimental design strategy for metabolic engineering. Metab. Eng. **3:** 124–137.

Phillips, I., and P. A. Silver, 2006 A new biobrick assembly strategy designed for facile protein engineering. In DSpace. MIT Artificial Intelligence Laboratory, MIT Synthetic Biology Working Group. http://hdl.handle.net/1721.1/32535.

Piper, M. D., S. P. Hong, G. E. Ball and I. W. Dawes, 2000 Regulation of the balance of one-carbon metabolism in *Saccharomyces cerevisiae*. J. Biol. Chem. **275:** 30987–30995.

Price, N., J. L. Reed, J. A. Papin, S. J. Wiback and B. O. Palsson, 2003 Network-based analysis of metabolic regulation in the human red blood cell. J. Theor. Biol. **225:** 185–194.

Quick, W. P., U. Schurr, R. Sheibe, E.-D. Schulze, S. R. Rodermel *et al.*, 1991 Decreased ribulose-1,5-bisphosphate carboxylase-oxygenase in tobacco transformed with 'antisense' *rbcS*. I. Impact on photosynthesis in ambient growth conditions. Planta **183:** 542–555.

Resendis-Antonio, O., R. J. Reed, S. Encarnacion, J. Collado-Vides and B. O. Palsson, 2007 Metabolic reconstruction and modeling of nitrogen fixation in *Rhizobium etli*. PLoS Comp. Biol. **3:** e192.

Rothermel, B. A., J. L. Thornton and R. A. Butow, 1997 Rtg3p, a basic helix-loop-helix/leucine zipper protein that functions in mitochondrial-induced changes in gene expression, contains independent activation domains. J. Biol. Chem. **32:** 19801–19807.

Schilling, C. H., D. Letsher and B. Ø. Palsson, 2000 Theoryfor the systemic definition of metabolic pathways and their use in interpreting metabolic function from a pathway-oriented perspective. J. Theor. Biol. **203:** 229–248.

Schuster, S., D. A. Fell and T. Dandekar, 2000 A general definition of metabolic pathways useful for systematic organization and analysis of complex metabolic networks. Nat. Biotechnol. **18:** 326–332.

Schuster, S., S. Klamt, W. Weckwerth, F. Moldenhaurer and T. Pfeiffer, 2002 Use of network analysis of metabolic systems in bioengineering. Bioproc. Biosyst. Eng. **24:** 363–372.

Shiba, Y., E. M. Paradise, J. Kirby, D. K. Ro and J. D. Keasling, 2007 Engineering of the pyruvate dehydrogenase bypass in *Saccharomyces cerevisiae* for high-level production of isoprenoids. Metab. Eng. **9:** 160–168.

Smith, R. L., and A. D. Johnson, 2000 Turning genes off by Ssn6-Tup1: a conserved system of transcriptional repression in eukaryotes. Trends Biochem. Sci. **25:** 325–330.

Sporty, J. L., M. M. Kabir, K. W. Turteltaub, T. Ognibene, S. J. Lin *et al.*, 2008 Single sample extraction protocol for the quantification of NAD and NADH redox states in Saccharomyces cerevisiae. J. Sep. Sci. **31:** 3202–3211.

Stein, I., Y. Peleg, S. Even-Ram and O. Pines, 1994 The single translation product of the FUM1 gene (fumarase) is processed in the mitochondria before being distributed between the cytosol and the mitochondria in Saccharomyces cerevisiae. Mol. Cell. Biol. **14:** 4770–4778.

Stelling, J., and E. D. Gilles, 2004 Mathematical modeling of complex regulatory networks. IEEE Trans. Nanobioscience **3:** 172–179.

Stitt, M., W. P. Quick, U. Schurr, E.-D. Schulze, S. R. Rodermel *et al.*, 1991 Decreased ribulose-1,5-bisphosphate carboxylase-oxygenase in tobacco transformed with 'antisense' *rbcS*. II. Flux-control coefficients for photosynthesis in varying light, CO_2, and air humidity. Planta **183:** 555–566.

Subramanian, M., W. B. Qiao, N. Khanam, O. Wilkins, S. D. Der *et al.*, 2005 Transcriptional regulation of the one-carbon metabolism regulon in *Saccharomyces cerevisiae* by Bas1p. Mol. Microbiol. **57:** 53–69.

Swiegers, J. H., N. Dippenaar, I. S. Pretorius and F. F. Bauer, 2001 Carnitine-dependent metabolic activities in *Saccharomyces cerevisiae*: three carnitine acetyltransferases are essential in a carnitine-dependent strain. Yeast **18:** 585–595.

Tate, J. J., and T. G. Cooper, 2003 Tor1/2 regulation of retrograde gene expression in *Saccharomyces cerevisiae* derives indirectly as a consequence of alterations in ammonia metabolism. J. Biol. Chem. **38:** 36924–36933.

Teixeira, M. C., P. Monteiro, P. Jain, S. Tenreiro, A. R. Fernandes *et al.*, 2006 The YEASTRACT database: a tool for the analysis of transcription regulatory associations in *Saccharomyces cerevisiae*. Nucleic Acids Res. **34:** D446–D451.

Thomas, S., and D. A. Fell, 1996 Design of metabolic control for large flux changes. J. Theor. Biol. **182:** 285–298.

Thompson, J. R., J. K. Bell, J. Bratt, G. A. Grant and L. J. Banaszak, 2005 Vmax regulation through domain and subunit changes. The active form of phosphoglycerate dehydrogenase. Biochemistry **44:** 5763–5773.

van Maris, A. J., A. A. Winkler, D. Porro, J. P. van Dijken and J. T. Pronk, 2004 Homofermentative lactate production cannot sustain anaerobic growth of engineered *Saccharomyces cerevisiae*: possible consequence of energy-dependent lactate export. Appl. Environ. Microbiol. **70:** 2898–2905.

Varma, A., and B. O. Palsson, 1994 Metabolic flux balancing: basic concepts, scientific and practical use. Biotechnology **12:** 994–998.

Visser, D., G. A. van Zuylen, J. C. van Dam, M. R. Eman, A. Proll *et al.*, 2004 Analysis of in vivo kinetics of glycolysis in aerobic Saccharomyces cerevisiae by application of glucose and ethanol pulses. Biotechnol. Bioeng. **88:** 157–167.

Vogt, A. M., H. Nef, J. Schaper, M. Poolman, D. A. Fell *et al.*, 2002 Metabolic control analysis of anaerobic glycolysis in human hibernating myocardium replaces traditional concepts of flux control. FEBS Lett. **24:** 245.

Waks, Z., and P. A. Silver, 2009 Engineering a synthetic dual organism for hydrogen production. Appl. Environ. Eng. **75:** 1867–1875.

Waterman, M. R., and E. R. Simpson, 1989 Regulation of steroid hydroxylase gene expression is multifactorial in nature. Recent Prog. Horm. Res. **45:** 155–163.

Werle, M., J. Kreuzer, J. Höfele, A. Elsässer, C. Ackermann *et al.*, 2005 Metabolic control analysis of the Warburg-effect in proliferating vascular smooth muscle cells. J. Biomed. Sci. **12:** 827–834.

Wildermuth, M., 2000 Metabolic control analysis: biological applications and insights. Genome Biol. **1:** 1031.

Wu, M., and A. Tzagoloff, 1987 Mitochondrial and cytoplasmic fumarases in *Saccharomyces cerevisiae* are encoded by a single nuclear gene *FUM1*. J. Biol. Chem. **262:** 12275–12282.

Yoshida, A., T. Nishimura, H. Kawaguchi, M. Inui and H. Yukawa, 2005 Enhanced hydrogen production from formic acid by formate hydrogen lyase-overexpressing *Escherichia coli* strains. Appl. Environ. Microbiol. **71:** 6762–6768.

Zelle, R. M., E. de Hulster, W. A. van Winden, P. de Waard, C. Dijkema *et al.*, 2008 Malic acid production by *Saccharomyces cerevisiae*: engineering of pyruvate carboxylation, oxaloacetate reduction, and malate export. Appl. Environ. Microbiol. **74:** 2766–2777.

Communicating editor: S. Fields

GENETICS

Supporting Information

http://www.genetics.org/cgi/content/full/genetics.109.105254/DC1

Systems-Level Engineering of Nonfermentative Metabolism in Yeast

Caleb J. Kennedy, Patrick M. Boyle, Zeev Waks and Pamela A. Silver

DOI: 10.1534/genetics.109.105254

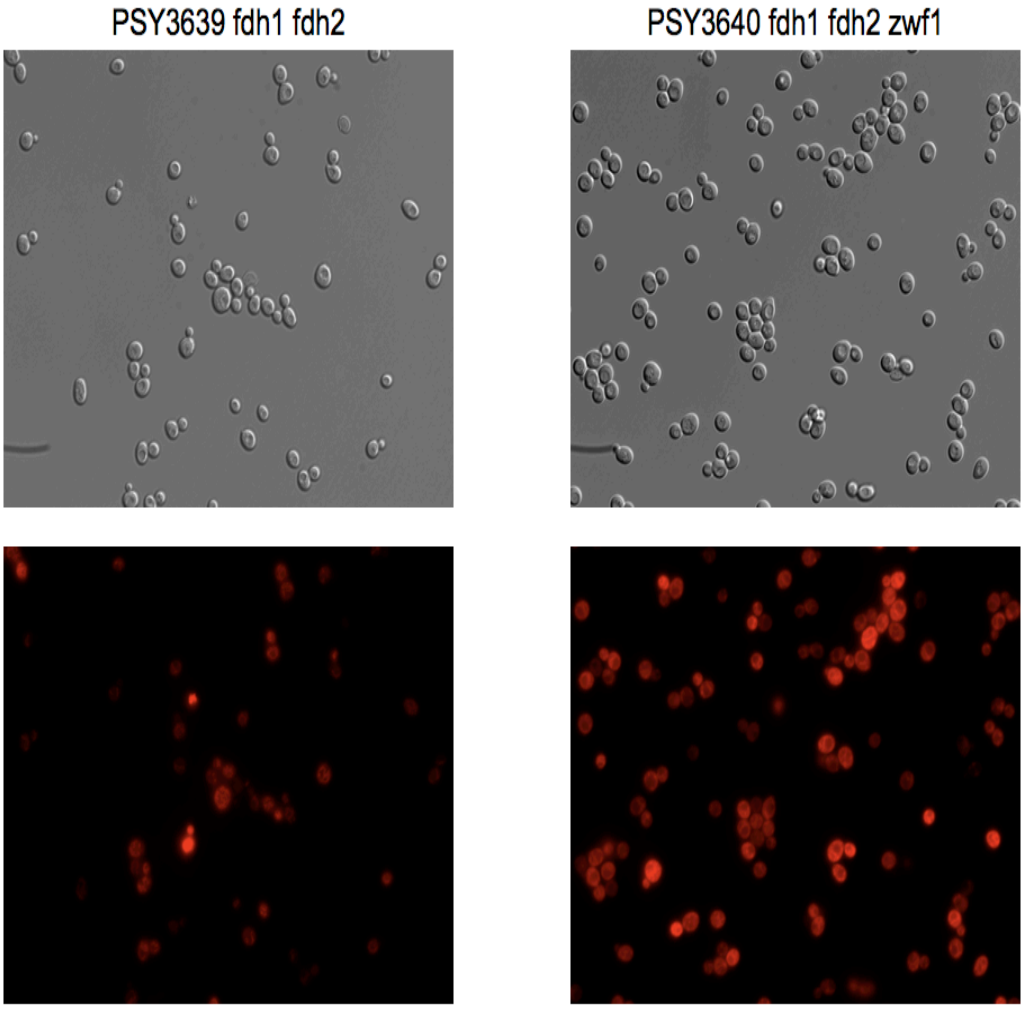
PSY3639 fdh1 fdh2
PSY3640 fdh1 fdh2 zwf1

PSY3653 fdh1 fdh2 fum1

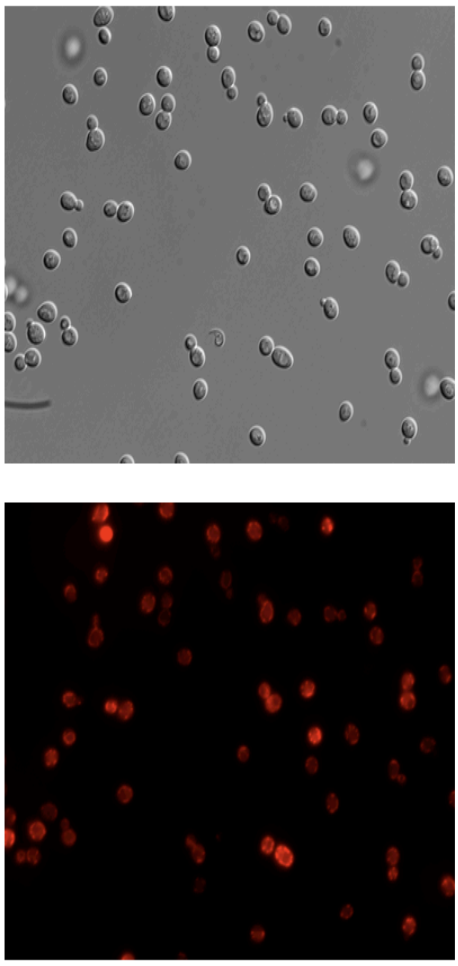

PSY3641 fdh1 fdh2 zwf1 fum1

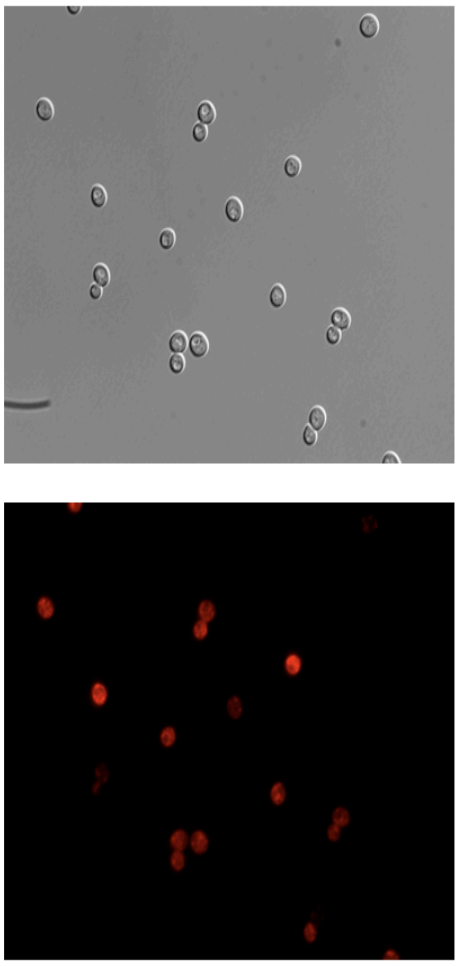

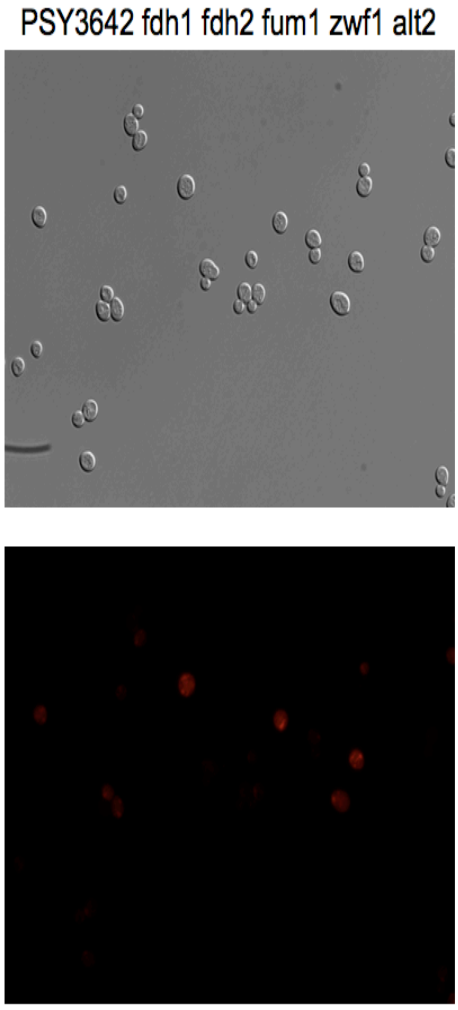

FIGURE S1.—Comparison of Mitotracker staining of strains described in this study. For each strain, the upper image is DIC at 60x magnification, and the lower image is the Mitotracker signal from the same field. Materials and methods are identical to the Mitotracker CMXRos protocol described in the main text.

TABLES S1-S4

Tables S1-S4 are available for download as Excel files at http://www.genetics.org/cgi/content/full/genetics.109.105254/DC1.